ISSN 1075-7015, Geology of Ore Deposits, 2022, Vol. 64, No. 7, pp. 503–512. © Pleiades Publishing, Ltd., 2022.
Russian Text © The Author(s), 2021, published in Zapiski Rossiiskogo Mineralogicheskogo Obshchestva, 2021, No. 1, pp. 63–75.

Indicator and Isotope Geochemical Characteristics of Iron Sulfides from the Golets Vysochaishy Deposit, East Siberia

Yu. I. Tarasova[a, b], *, A. E. Budyak[a, b], A. V. Ivanov[c], N. A. Goryachev[a, d], A. V. Ignatiev[e], T. A. Velivetskaya[e], T. A. Radomskaya[a], A. V. Blinov[a], and V. N. Babyak[a]

[a] *Vinogradov Institute of Geochemistry, Siberian Branch, Russian Academy of Sciences, Irkutsk, 664033 Russia*

[b] *Irkutsk National Research Technical University, Irkutsk, 664074 Russia*

[c] *Institute of the Earth's Crust, Siberian Branch, Russian Academy of Sciences, Irkutsk, 664033 Russia*

[d] *Northeastern Interdisciplinary Research Institute, Far East Branch, Russian Academy of Sciences, Magadan, 685000 Russia*

[e] *Far East Geological Institute, Far East Branch, Russian Academy of Sciences, Vladivostok, 690022 Russia*

**e-mail: j.tarasova84@yandex.ru*

Received October 13, 2020; revised October 23, 2020; accepted December 10, 2020

Abstract—This paper provides new data on various pyrite and pyrrhotite generations at the Golets Vysochaishy gold deposit, Bodaibo district, Irkutsk Oblast. These generations are distinguished by morphological, geochemical, and isotope ($\delta^{34}S$) features. The established features of pyrite generations reflect the evolution of the Golets Vysochaishy deposit. Each pyrite generation is associated with a certain evolutionary stage of Neoproterozoic rocks in the region: (1) diagenesis (610 Ma), (2) catagenesis (570–520 Ma), (3) metamorphism (~450–430 Ma), and (4) tectono-magmatic activation (330–270 Ma). The $^{40}Ar/^{39}Ar$ ages of the third and fourth pyrite generations correspond to those of previously determined gold mineralization and granite magmatism.

Keywords: indicator features, pyrite, pyrrhotite, sulfur isotopes, dating, gold deposits, Baikal–Patom Highlands, East Siberia

DOI: 10.1134/S1075701522070108

INTRODUCTION

The Lena Province is one of the largest in the number of gold deposits and their total reserves, not only in Russia, but worldwide. Here are the Sukhoi Log giant deposit; the large Golets Vysochaishyi, Verninskoe, Ugakhan, Krasny, Svetlovskoe, and Ykan deposits; and some other smaller primary and placer deposits.

Compared to the quite well-documented Sukhoi Log (Distler et al., 1996; Buryak and Khmelevskaya, 1997; Laverov et al., 2007, Large et al., 2007; Meffre et al., 2008; Rusinov et al., 2008; Kryazhev et al., 2009; Chernyshev et al., 2009; Yudovskaya et al., 2011, 2016; Chugaev et al., 2014), the Golets Vysochaishyi deposit, located 30 km northeast of Sukhoi Log and its closest analogue, is the clearly understudied (Vagina, 2012; Kucherenko et al., 2012). This paper provides new data on indicator features and the chemical and sulfur isotopic composition of pyrite and pyrrhotite as the major ore minerals at this deposit. This has made it possible to establish the formation sequence of various sulfide generations and supplement knowledge on the evolution of the ore-forming processes in the Bodaibo district as a whole.

ANALYTICAL TECHNIQUES

The relationships of minerals and primary textures of grains were studied using identification etching of iron sulfides. Pyrite and pyrrhotite were exposed for 10–40 s to concentrated nitric and hydrochloric acid, respectively.

The ore mineralogy was study with both optical method (polarizing microscope Olympus BX-51) and electron probe microanalysis (a JXA8200 JEOL electron microprobe equipped with five wave dispersion and energy dispersion (EX84055MU) spectrometers). Operation conditions at electron probe microanalysis (EPMA) were: 20 kV acceleration voltage and 25 nA current intensity. Pyrite and pyrrhotite were studied in two modes: (1) electron microscopy in secondary and backscattered electrons and X-ray mapping, and (2) quantitative microanalysis using wave dispersion spectrometers with the LDE1, LDE2, TAP, TAPH, PET, PETH, LiF, and LiFH crystals.

Sulfur isotopic composition was measured using an NWR Femto femtosecond laser ablation instrument at the Laboratory of Stable Isotopes at the Resource Center in the Far East Geological Institute, Far East Branch, Rusisan Academy of Sciences (Ignatiev et al.,

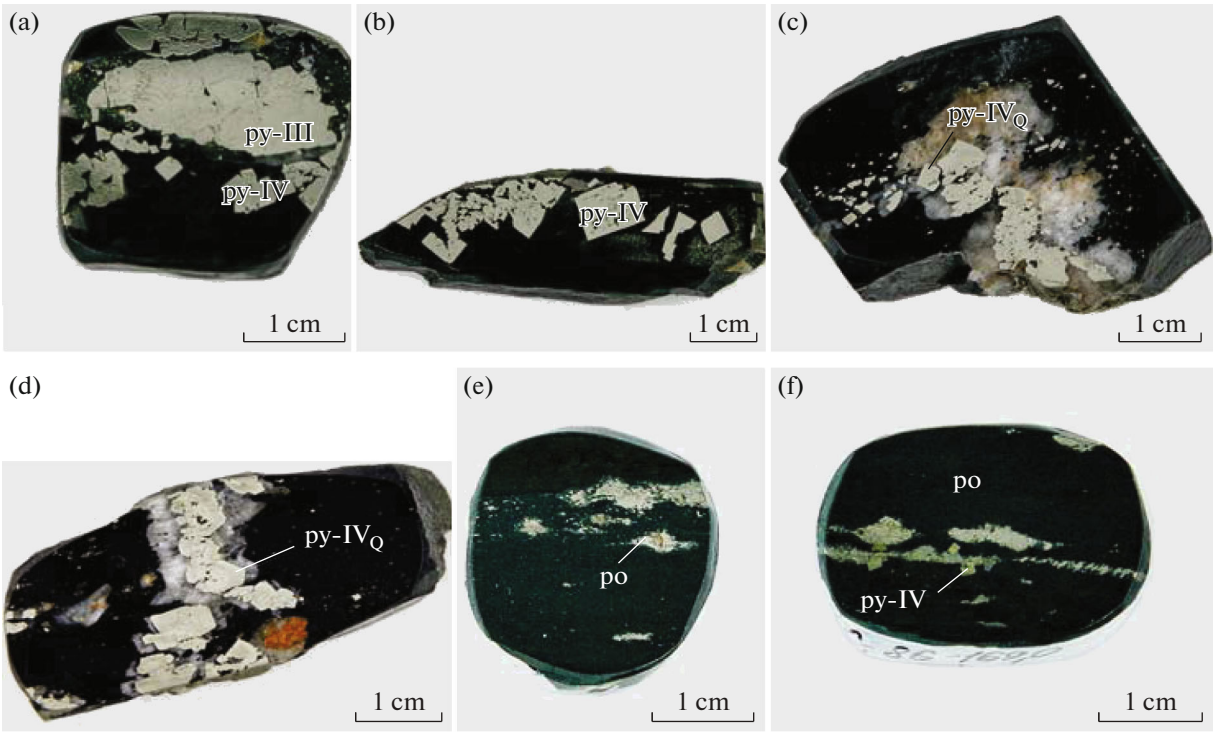

Fig. 1. Relationships of pyrite (py) and pyrrhotite (po) typical of Golets Vysochaishiy deposit. (I, II, IV, IV$_Q$) pyrite generations.

2018; Velivetskaya et al., 2019). The sulfur isotope ratio was measured for masses of 127 ($^{32}SF^{5+}$) and 129 ($^{34}SF^{5+}$) using a MAT-253 (Thermo Fisher Scientific) mass spectrometer. The measurements were conducted on a laboratory standard calibrated in accordance with the international standards IAEA-S-1, IAEA-S-2, and IAEA-S-3. The measured $\delta^{34}S$ values are given in relation to the VCDT international standard and are expressed in per mille (‰). The analytical accuracy in determining $\delta^{34}S$ was ±0.20‰ (2σ).

$^{40}Ar/^{39}Ar$ dating was performed on an ARGUS VI mass spectrometry complex consisting of an ARGUS VI mass spectrometer (Thermo Fisher Scientific), gas purification unit, and double vacuum high-vacuum-resistant furnace. The procedure is described in detail in (Ivanov et al., 2015). The IsoplotR program (Vermeesch, 2018) was used to construct the step heating diagram.

OBJECT OF STUDY

The Golets Vysochaishy deposit, situated in Irkutsk oblast, is located on the western flank of the Bodaibo synclinorium within the deformed structures of the southern passive margin of the Siberian Craton (SC) (Ivanov, 2014). Neproterozoic terrigenous–carbonate host rocks were green schist facies metamorphosed (Perov and Makrygina, 1975; Stanevich et al., 2007; Nemerov et al., 2010; Ivanov, 2014). Most gold occurrences are hosted by the sericite–chlorite subfacies rocks.

The deposit is structural related to the foot limb of the Kamenka near EW anticline fold. Rhythmic intercalated dark gray moderate carbonaceous (1.0–1.5 to 7.2% C_{org}) sandstone, siltstone, and pelite belong to the lower subformation of the Khomolkho Formation are the host rocks. These rocks contain abundant ankerite and are underlain by carbon-bearing terrigenous–carbonate and terrigenous sediments of the Ugakhan and Buzhuikhta formations, respectively, constituting the core of the Kamenka anticline (Buryak and Khmelevskaya, 1997; Ivanov, 2014).

The mineralized zone is delineated by the 0.4 g/t cutoff grade at the deposit and comprises two orebodies (western and eastern) with complex morphology and total extension ~3000 m. The mineralized zone is EW striking and N dipping at 5°–10°, which is close to the rock stratification (Buryak and Khmelevskaya, 1997). The gold reserves at the deposit are 81 tons (Babyak et al., 2020).

Pyrite and pyrrhotite are the major ore minerals of the Golets Vysochaishy deposit (Fig. 1). Galena, chalcopyrite, and sphalerite are subordinate. Native gold as interstitial particles is associated with pyrite and less frequent pyrrhotite, galena, chalcopyrite, and sphalerite.

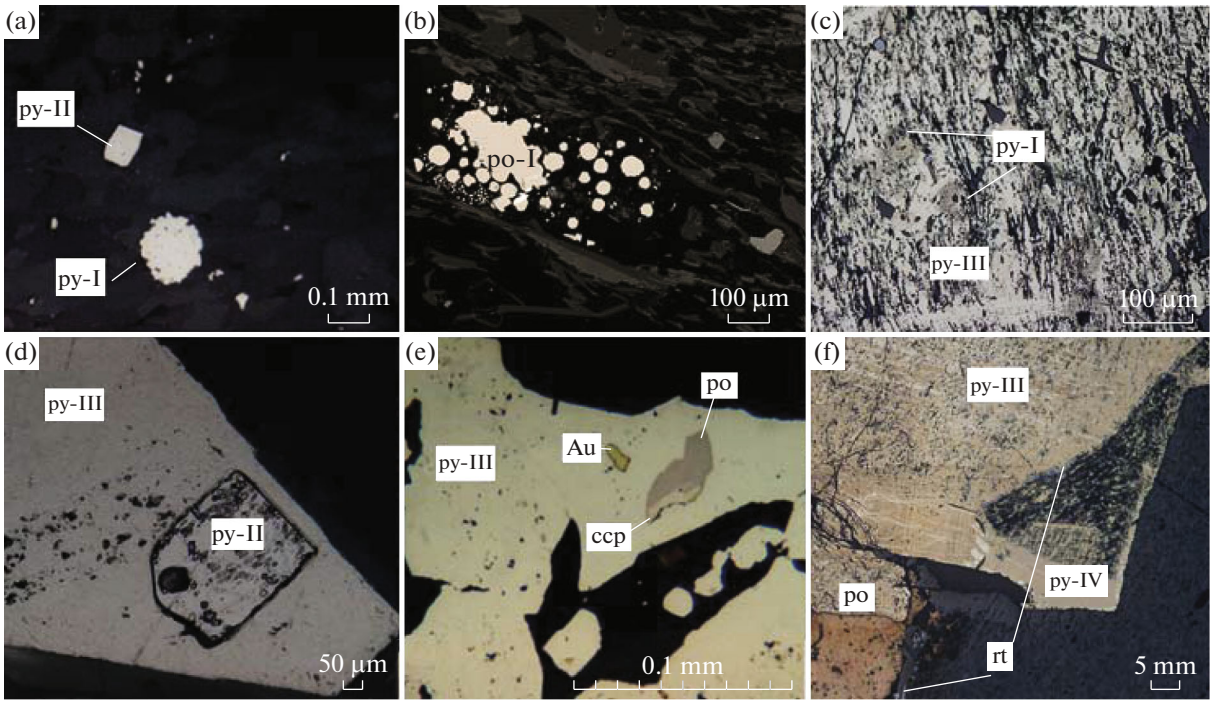

Fig. 2. Pyrite generations. (a) Pyrite I and pyrite II grains; (b) cluster of framboidal pyrrhotite-II in host rocks; (c) relict pyrite-I crystals in metaaggregate of pyrite-III (after etching); (d) relict pyrite-II cubes in the pyrite III aggregate (photomicrograph after identification etching); (e) pyrite III meta-aggregate with inclusions of chalcopyrite, pyrrhotite and native gold; (f) aggregate of the veinlet-like pyrrhotite segregation and pyrite IV crystal, and the rutile rim along pyrrhotite and pyrite III. Pyrite, py; pyrrhotite, po; chalcopyrite, ccp, rutile, rt; native gold, Au.

RESULTS

At the Golets Vysochaishy deposit, four pyrite generations are distinguished, differing in morphology, relationships with mineral assemblages, and chemical and isotope composition.

The earliest generation (pyrite I) is observed as framboids or oval clusters in host rocks (Figs. 2a, 2b). Such segregations do not exceed 120 μm in size. Relics of pyrite I (visible after identification etching) are quite common in later pyrite generations (Fig. 2c). Framboidal pyrite I grains are enclosed in aggregates of pyrite III (Fig. 2e) or euhedral pyrite IV crystals in host rocks. In addition, framboidal pyrrhotite grains presenting pseudomorphs after pyrite I were identified (Fig. 2b); this indicates the earlier pyrite I precipitation. The composition of various pyrite generations has been studied with EPMA (Table 1). Relict pyrite I enclosed in pyrite IV is characterized by the elevated gold background (Fig. 4); the Au content reaches 0.14 wt %. In addition to gold, pyrite I contains minor Co and Ni with a predominance of the latter.

Fine cubes of pyrite II (Fig. 2d) are usually disseminated in host rocks and are more frequently in the sandstone intercalations. Euhedral pyrite II crystals do not exceed 200 μm in size. The crystal surface is uniform; edges are smooth. Relics of pyrite I are observed in pyrite II. As a result of identification etching, relics of pyrite II were established in pyrite III (Fig. 2d), pyrite IV (Fig. 3b), and pyrrhotite aggregates (Fig. 3e). On the surface of pyrite II, gold is distributed similar to that of pyrite I and its concentration is comparable (Table 1). Pyrrhotite pseudomorphs after pyrite II cubes with non-stoichiometric sulfur content (Fig. 3, Table 1) are identified using EPMA. The size of these crystals is approximately 200 μm.

Pyrrhotite replacing early pyrite generations forms large lenticular and short veinlet-like banded segregations concordant to foliation of host rocks (Figs. 1e, 1f). Long zones with linear moderate and dense dissemination of equant and elongated-equant pyrrhotite segregations are also present. The pyrrhotite grain size is fractions of a millimeter; the length of its veinlet-type and lenticular segregations is a few cm; the thickness does not exceed 2–4 mm as a rule. Boundaries with host rocks are scalloped and curved.

The formation of pseudomorphs after framboidal pyrite I (Fig. 3b) and cubic pyrite II (Figs. 3e, 3f) has been confirmed. Later aggregates of pyrite III contain rounded inclusions of pyrrhotite entrapped during growth (Fig. 2e). Occasionally, minor Ni, typical of pyrite I, occurs as an individual phase as result of pyrrhotite pseudomorph formation (Fig. 2b). Partial pyrrhotite pseudomorphs after pyrite II crystals are observed in pyrrhotite aggregates; therefore, the chemical composition of such pseudomorphs is transitional with the higher elevated Fe content (52.48–

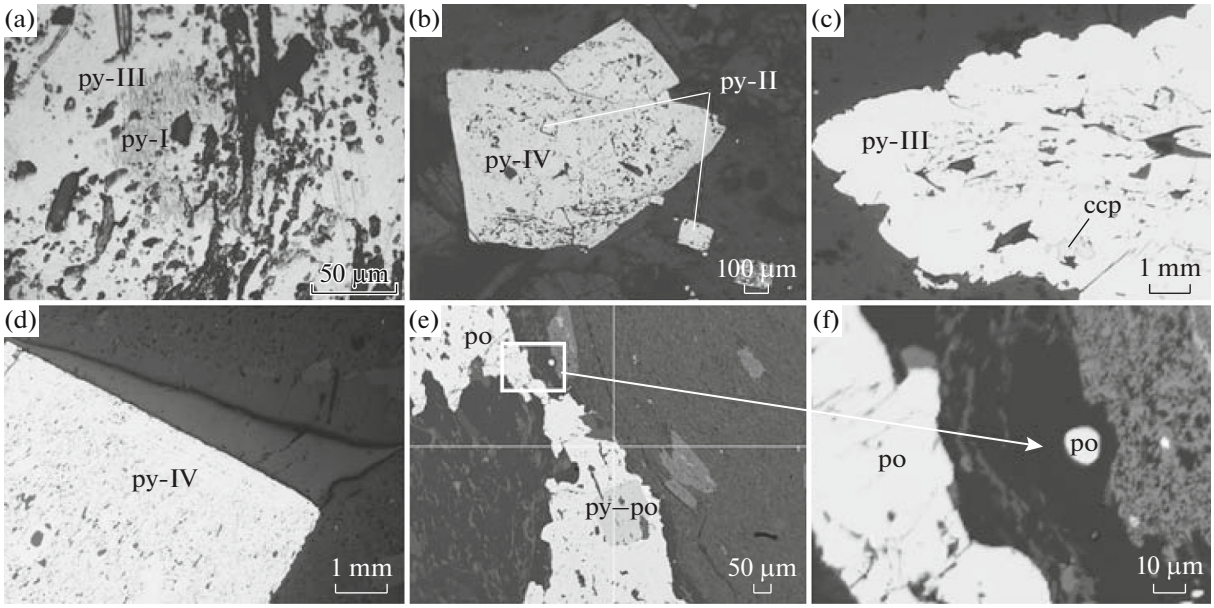

Fig. 3. Pyrite generations whose compositions were determined by EPMA. See Fig. 2 for mineral abbreviations.

56.75 wt %) than that of unaltered pyrite II (Fig. 3e, Table 1).

The third pyrite generation (pyrite III) is isometric elongated aggregates. The thickness of a series of banded granular pyrite III segregations ranges from 0.5 to 2–3 cm, whereas that of individual linear veinlets does not exceed 1–2 mm. The size of pyrite aggregates varies from a few portions of mm to 1–2 cm. Pyrite is sievelike, poikilitic, and slightly fractured. Pyrite III aggregates are saturated in fine rounded pyrrhotite inclusions replacing pyrite I and II (Fig. 1e). Pyrite III contains considerable inclusions of gangue minerals (predominantly quartz). Pyrite III is associated with sulfides of polymetallic assemblage (chalcopyrite, pyrrhotite, sphalerite, galena) and native gold,

Table 1. Electron microprobe data (wt %) and $\delta^{34}S$ values (‰) for pyrite of various generations from Golets Vysochaishiy deposit

Pyrite generations	Fe	S	As	Co	Ni	Au	$\delta^{34}S$
Pyrite I	44.25(5) 43.8–44.7	54.20(5) 53.3–54.9	–	0.13(5) 0.10–0.16	0.15(5) 0.0–0.20	0.14(5) 0.11–0.20	–
Pyrite II	45.58(7) 45.11–46.69	53.74(7) 52.39–54.13	–	–	–		–
Pyrrhotite	60.11(41) 56.04–61.06	39.09(41) 37.53–39.88	–	–	–	–	4.2(15) 3.8–4.6
Pyrite III	46.81(11) 46.58–47.07	53.14(11) 52.78–53.68	–	–	–	–	7.6(11) 6.3–8.7
Pyrite IV	46.38(17) 46.00–46.67	53.41(17) 53.14–53.73	0.29(17) 0.26–0.31	–	–	–	6.5(26) 5.3–7.3
Pyrite IV_Q	46.24(13) 46.11–46.73	53.53(13) 53.21–53.80	0.33(13) 0.19–0.42				6.6(15) 5.8–7.3

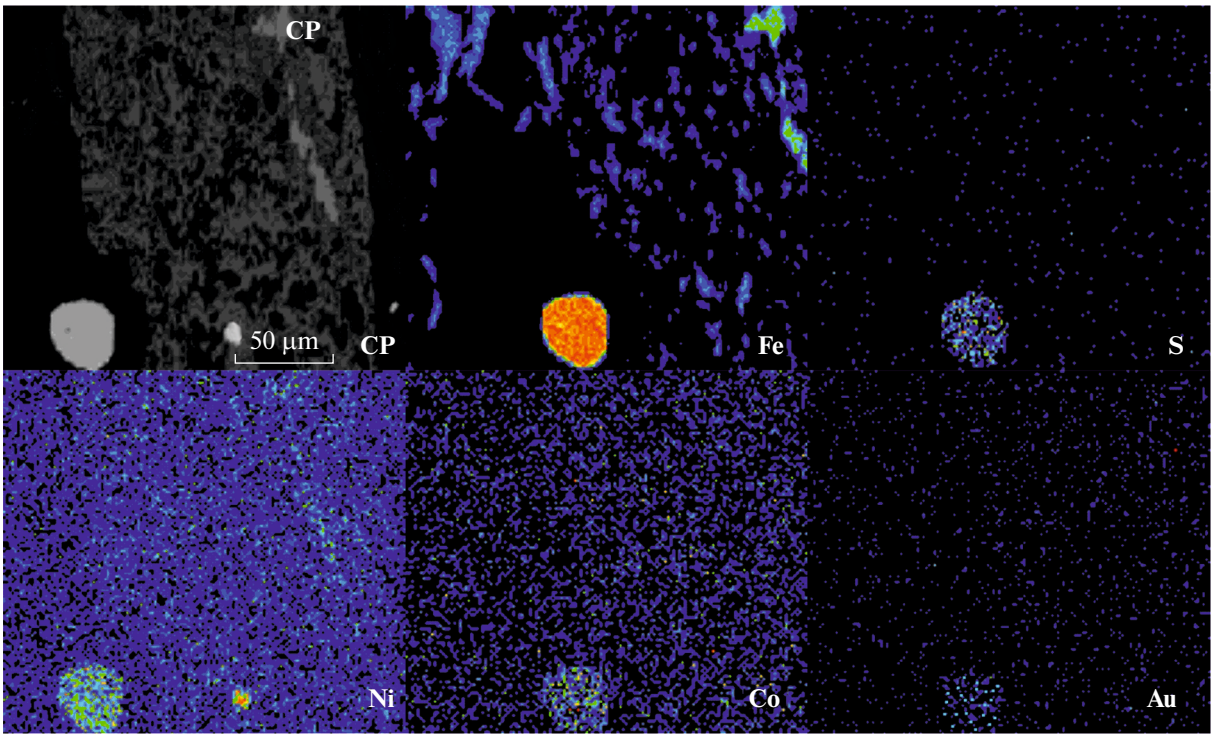

Fig. 4. X-ray distribution maps of Fe, S, Ni, Co, and Au in pyrite I.

which fill fractures and interstices in pyrite III aggregates and rim them. At the Golets Vysochaishy deposit, economic gold grade is associated with large aggregates of pyrite III (Ivanov, 2014). Despite many inclusions of sulfides and native gold, pyrite III is devoid of minor elements (Table 1).

Pyrite IV is the latest pyrite generation. It occurs as large (up to 2 cm) cubes with distinct faces. The pyrite IV crystals are confined to the rim of milky-white quartz of 2–3 mm thick. Pyrite IV forms isolated crystals in host rocks or overprints pyrite III crystals to form cubes.

Pyrite from the late quartz–sulfide veinlets was studied separately. Veinlets of milky-white quartz up to 0.5 cm thick cut host rocks and pyrite III aggregates, but not pyrite IV. Similar morphology of pyrite of veinlets and pyrite IV suggests their attribution to the same generation; therefore, pyrite from quartz veins is marked as pyrite IV_Q. Accordingly, quartz veinlets are simultaneous with disseminated pyrite IV.

Pyrite from the late crosscutting veinlets occurs as lenticular pods concordant to the foliation at the contact of quartz and host rocks. These aggregates are composed of cubic crystals. In contrast to other generations, pyrite IV and pyrite IV_Q contain gold as neither surface impurity nor inclusions of native metal. Only minor As (up to 0.3 wt %) was measured in pyrite IV and pyrite IV_Q crystals (Table 1).

ISOTOPE DATA

The small size of the pyrite I and II grains and replacement of them by pyrrhotite prevented their isotope study. The $\delta^{34}S$ value of pyrrhotite replacing pyrite I and II ranges from +3.8 to +4.6‰ (average +4.2‰). Pyrite III has the heaviest sulfur with the deposit, $\delta^{34}S$ +6.3...+8.7‰, average +7.6‰. Sulfur isotopic composition of pyrite IV $\delta^{34}S$ +5.3...+7.3‰, average +6.5‰) and pyrite IV_Q (($\delta^{34}S$ +5.8...+7.3‰, average +6.6‰) falls between values for pyrrhotite and pyrite III (Fig. 5, Table 1).

The $^{40}Ar/^{39}Ar$ dating of pyrite denotes dating of potassium-bearing inclusions, usually sericite (Ivanov et al., 2015). Given that there are few such inclusions, the dates obtained have large measurement uncertainty. Nevertheless, the dated pyrite III and IV samples are statistically different in their plateau age. For example, pyrite III sample KZ-8/7 was dated at the plateau age of 437 ± 62 Ma for the six temperature steps, during which more than 90% of ^{39}Ar were released (Fig. 6a). The isochron age is consistent with the plateau age within even greater uncertainty. The initial isotope ratio of entrapped argon ($^{40}Ar/^{36}Ar_0$) is consistent with air argon ($^{40}Ar/^{36}Ar_0 = 298.56$) within the measurement uncertainty (Lee et al., 2006) and makes it possible to take the plateau age as the dating. Similarly, the pyrite IV sample yielded a significant

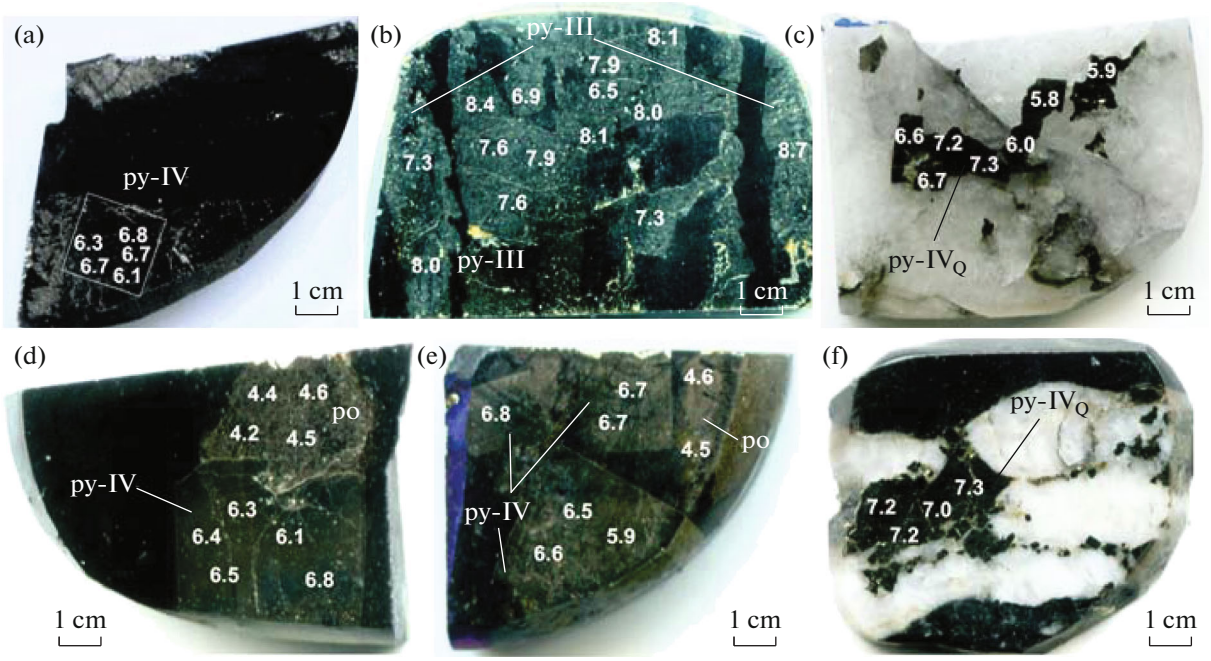

Fig. 5. Variations in sulfur isotopic composition of pyrite and pyrrhotite from Golets Vysochaishy deposit.

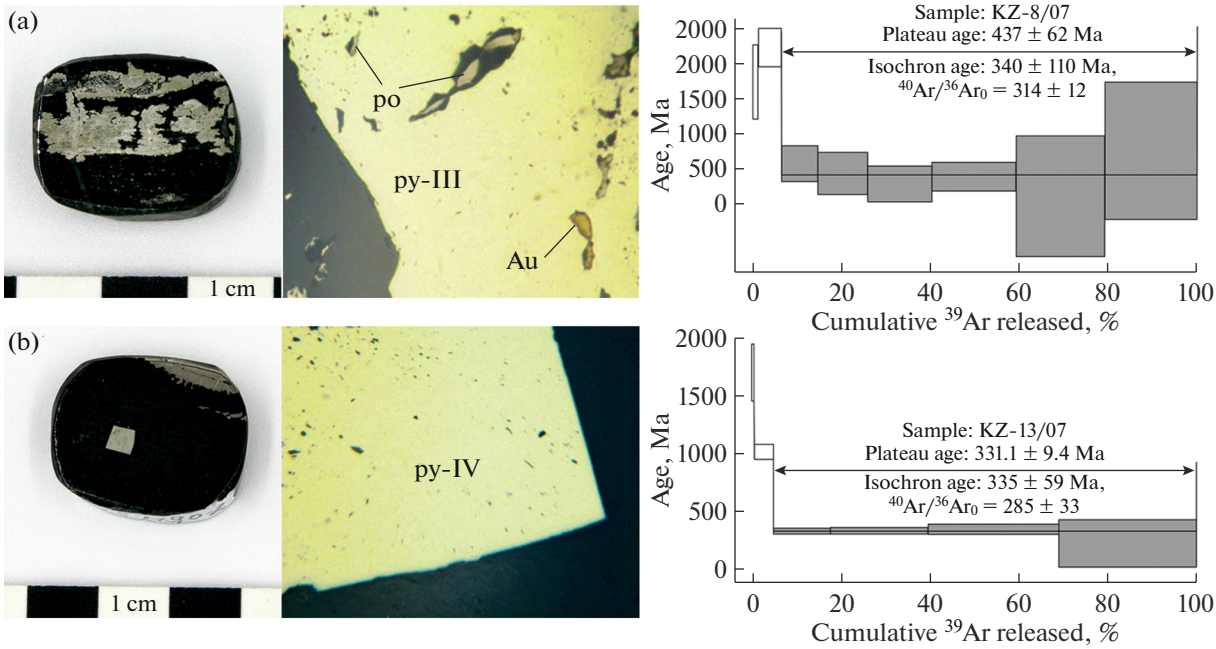

Fig. 6. $^{40}Ar/^{39}Ar$ step heating spectra of samples studied: (a) pyrite III and (b) pyrite IV, for which general view and photomicrographs in reflected light are presented.

value of plateau age, 331 ± 9 Ma (Fig. 6b). This pyrite also shows entrapped atmospheric argon ($^{40}Ar/^{36}Ar_0$).

DISCUSSION

The pyrite–pyrrhotite mineralization sequence at the Golets Vysochaishy deposit in its key characteristics is consistent with the previously reported mineralization sequence at the Sukhoi Log and Krasnoe deposits (Large et al., 2007; Tarasova et al., 2020). This indicates similar scenario for ore-forming processes. We attributed pyrite I to diagenetic as evidenced by the following facts: the thinnest rounded grains with a slight sulfur excess (up to 54.2 wt %) and

minor Co and Ni with the latter predominance that is typical of diagenetic pyrite (Ramdohr, 1959; Hamor, 1994; Chvileva et al., 1988; Xu et al., 2020). Gold admixture on the crystal surface of pyrite I is due to co-precipitation of Au, Fe and S during pyrite formation (Tauson et al., 2009) at the stage of diagenetic transformation of sediments.

The pyrite II composition is close to stoichiometric. Euhedral pyrite crystals are formed at temperatures from 150–200°C (Yapaskurt, 2005). This agrees with the catagenetic stage of terrigenous rocks of the Dal'nyaya Taiga–Zhuya Group within the Bodaibo synclinorium (Nemerov et al., 2010). Extensive replacement of pyrite I and II by pyrrhotite (Kretschmar and Scott, 1976; Hall, 1986) at the preore stage of the deposit is associated with a beginning of progressive metamorphism of sedimentary sequences during great thermal fluid event. Abundant pyrrhotite indicates the higher-grade metamorphism at the Golets Vysochaishy deposit than at the surrounding gold deposits including Sukhoi Log. According to Goryachev et al. (2019), this is caused by the closeness of Golets Vysochaishy to the cores of areas of thermal influence resulted from zoned granite-metamorphic cupola within the Bodaibo Synclinorium (Mama-Oron metamorphic belt) dated at the late Early Paleozoic (450–420 Ma) (Zorin et al., 2008; Yudovskaya et al., 2011). Thus, abundant pyrrhotite is a mineralogical indicator for separation of early and late pyrite generations.

Pyrite III typical of the are stage at the deposit is intimately associated as rule with pyrrhotite. According to Hamor (1994), massive irregularly shaped aggregates similar to those of pyrite III are formed under open system conditions with abrupt pressure decreasing and inflow of fluid enriched in sulfur into the mineralized system. Accordingly, pyrite III may be attributed to the retrograde geodynamic stage of the Badaibo district.

This is supported by the pyrite III age (437 ± 62 Ma) (Fig. 6a) that is consistent with both the ore dating at the Sukhoi Log deposit (450–440 Ma) and metamorphic transformations in the Late Ordovician to Silurian (~450–420 Ma) (Laverov et al., 2007; Meffre et al., 2008; Yudovskaya, 2011; Chugaev et al., 2014).

The fourth pyrite generation overprinting all previous pyrite–pyrrhotite generations with the deposit testifies to the tectonic activation in the region. The arsenic admixture on the surface of pyrite IV crystals indicates their interaction with fluid enriched in As. In turn, the input of As in the fluid is possible through the redistribution of chemical elements from the earlier mineral assemblages at the low- to mid-temperature postmineralization stage (<200°C) of the deposit formation.

The obtained $^{40}Ar/^{39}Ar$ date of pyrite IV, 331 ± 9 Ma (Fig. 6b), is close to the Rb-Sr dates of late hydrothermal veins at the Sukhoi Log deposit, 321 ± 14 Ma (Laverov et al., 2007). This age range is consistent with that of polychronous Angara–Vitim batholith emplacement (340–320 to 310–270 Ma) (Bukharov et al., 1992; Neimark et al., 1993; Tsygankov, 2005). The Konstantinovsky biotite granite pluton belonging to the Konkudera–Mamakan Complex (300 ± 20 Ma) (Neimark et al., 1993) is the closest to the Sukhoi Log and Golets Vysochaishy deposits.

Variations in sulfur isotopic composition

The sulfur isotopic composition of pyrrhotite replacing early pyrite–pyrrhotite generation and the third and fourth pyrite generations is different. Based on ideas from (Cook and Hoefs, 1997), we suggest insignificant homogenization of sulfur isotopic composition. Thus, the obtained $\delta^{34}S$ value of pyrrhotite (+3.8 to +4.6‰, average 4.3‰) may correspond to that of early pyrite with a certain degree of conditionality. This value is within the range of $\delta^{34}S$ of both sulfides of the Khomolkho Formation not affected by the mineralization process (+3.4‰) (Chugaev et al., 2018) and pyrite from the Ediacaran orogenic gold deposits over the world (+2 to +15‰) (Chang et al., 2008).

The heavier sulfur isotopic composition pyrite in pyrite III (+6.3 to +7.8‰, average +7.6‰) than that of pre-ore pyrrhotite could have resulted from the evolution of mineralizing fluid during metamorphic redistribution (Goryachev et al., 2019) or the effect of additional fluid with heavier sulfur derived from the deeper strata. The second version is supported by the fact that the average $\delta^{34}S$ of pyrite from the underlying Buzhuikhta Formation is +10.8‰ (Chugaev et al., 2018).

The obtained $\delta^{34}S$ of pyrite IV and IV_Q (average 5.9 and 6.6‰, respectively) is slightly lower than that of pyrite III, which implies no fluid exchange between various stratigraphic horizons at the late stage of the deposit in the Carboniferous to Early Permian.

Thus, the revealed morphological, compositional, and isotope features of pyrite generations reflect the evolution of the Golets Vysochaishy system. The precipitation of carbonaceous sediments with siderophile geochemical specialization (610–580 Ma) (Meffre et al., 2008; Powerman et.al., 2015; Budyak et al., 2016, 2019) can be considered the initial stage of the mineralization process. During this stage, pyrite I enriched in Au was formed. Pyrite II precipitated under increased PT parameters of the system as result of regional catagenetic low-grade alterations dated at 570–540 Ma (Mefre et al., 2008; Nemerov et al., 2010; Yudovskaya et al., 2011; Tarasova et al., 2020). The $\delta^{34}S$ of pyrrhotite replacing pyrite I and II is over the range of sulfur isotope composition of host sedimentary rocks of the Khomolkho Formation indicates that the host rocks were source for sulfur during pyrrhotite formation.

Ore-stage pyrite III was formed as a result of metamorphic transformation in Late Ordovician to Silurian (~450–420 Ma) (Laverov et al., 2007; Meffre et al., 2008; Yudovskaya et al., 2011; Chugaev et al., 2014). The higher $\delta^{34}S$ value of pyrite III is most likely resulted from input of heavier sulfur derived from underlain sediments of the Buzhuikhta Formation.

Postore pyrite IV dated at ~330 Ma was formed during tectonic activation that is consistent with an emplacement of the Angara–Vitim batholith (330–275 Ma) (Neimark et al., 1993; Tsygankov et al., 2010).

CONCLUSIONS

(1) The pyrite–pyrrhotite mineralization at the Golets Vysochaishy deposit evolved during four noncoeval stages; this is comparable with other objects in the Bodaibo region such as Sukhoi Log and Krasnoe (Large et al., 2007; Mefre et al., 2008; Palenova et al., 2015; Tarasova et al., 2020).

(2) Dating of the ore and postore stages (437 ± 62 and 331 ± 9 Ma, respectively) agrees with that suggested for the Sukhoi Log deposit (~450 and 320 Ma) (Laverov et al., 2007).

(3) Pyrite III, the major gold carrier, was formed from a fluid derived from rocks of the Buzhukhta Formation, which underlies rocks of the Khomolkho Formation hosting the deposit.

ACKNOLWEDGMENTS

The data presented in this study were obtained with equipment at the Resource Center Isotope and Geochemical Studies of the Vinogradov Institute of Geochemistry, Siberian Branch, Russian Academy of Sciences. The $^{40}Ar/^{39}Ar$ dating was performed at the Geodynamics and Geochronology Resource Center, Institute of Earth's Crust, Siberian Branch, Russian Academy of Sciences. The sulfur isotope composition was measured at the Laboratory of Stable Isotopes at the Resource Center of Far East Geological Institute, Far East Branch Russian Academy of Sciences.

FUNDING

The study was carried out within state order IX.130.3.1. (project no. 0350-2019-0010).

CONFLICT OF INTEREST

The authors declare that they have no conflicts of interest.

REFERENCES

Babyak, V.N., Blinov, A.V., Tarasova, J.I., and Budyak, A.E., New data on the geological and structural features of the Ozhereliye, Ykanskoye, Ugahan and Golets Vysochaishy gold fields, *Earth Sci. Subsoil Use*, 2019, vol. 42, no. 4, pp. 388–412.

Budyak, A.E., Goryachev, N.A., and Skuzovatov, S.Y., Geodynamic background for large-scale mineralization in the southern environs of the Siberian Craton in the Proterozoic, *Dokl. Earth Sci.*, 2016, vol. 470, no. 2, pp. 1063–1066.

Budyak, A.E., Skuzovatov, S.Yu., Tarasova, Yu.I., Wang, K.-L., and Goryachev, N.A., Common Neoproterozoic–Early Paleozoic evolution of ore-bearing sedimentary complexes in the southern Siberian craton, *Dokl. Earth Sci*, 2019, vol. 484, no. 1, pp. 92–96.

Bukharov, A.A., Khalilov, V.A., Strakhov, T.M., and Chernikov, V.V., Geology of the Baikal-Patom upland based on new data of U-Pb dating of accessory zircons, *Russ. Geol. Geophys*, 1992, no. 12, pp. 29–39.

Buryak, V.A. and Khmelevskaya, N.M., *Sukhoi Log—odno iz krupneishikh zolotorudnykh mestorozhdenii mira (genesis, zakonomernosti razmeshcheniya orudeneniya, kriterii prognozirovaniya* (Sukhoi Log is One of the World's Largest Gold Deposits (Genesis, Patterns of Mineralization Distribution, and Forecasting Criteria), Vladivostok: Dalnauka, 1997.

Chang, Z.S., Large, R.R., and Maslennikov, V.V., Sulfur isotopes in sediment-hosted orogenic gold deposits: evidence for an early timing and a seawater sulfur source, *Geology*, 2008, vol. 36, pp. 971–974.

Chernyshev, I.V., Chugaev, A.V., Safonov, Y.G., Saroyan, M.R., Yudovskay, M.A., and Eremina, A.V., Lead isotopic composition from data of high-precession MC-ICP-MS and sources of matter in the largescale Sukhoi Log noble metal deposit, Russia, *Geol. Ore Deposits*, 2009, vol. 51, no. 6, pp. 496–504.

Chugaev, A.V., Budyak, A.E., Chernyshev, I.V., Dubinina, E.O., Shatagin, K.N., Tarasova, Y.I., Skuzovatov, S.Y., Gareev, B.I., and Goryachev, N.A., Isotopic (Sm–Nd, Pb–Pb, and $\delta^{34}S$) and geochemical characteristics of the metasedimentary rocks of the Baikal–Patom belt (Northern Transbaikalia) and evolution of sedimentary basin in the Neoproterozoic, *Petrology*, 2018, vol. 26, no. 3, pp. 213–245.

Chugaev, A.V., Plotinskay, O.Yu., Chernyshev, I.V., and Kotov, A.A., Lead isotope heterogeneity in sulfides from different assemblages at the Verninsky gold deposit (Baikal–Patom highland, Russia), *Dokl. Earth Sci*, 2014, vol. 457, no. 1, pp. 887–892.

Chvileva, T.N., Bezsmertnaya, M.S., Spiridonov, E.M., Agroskin, A.S., Papayan, G.V., Vinogradova, R.A., Lebedeva, S.I., Zavyalov, E.N., Filimonova, AA., Petrov, V.K., Rautian, L.P., and Sveshnikova, O.L., *Spravochnik-opredelitel's rudnykh mineralov v otrazhennom svete* (Reference Book-Identifier of Ore Minerals in Reflected Light) Moscow: Nedra, 1988.

Cook, N.J. and Hoefs, J., Sulphur isotope characteristics of metamorphosed Cu–(Zn) volcanogenic massive sulphide deposits in the Norwegian Caledonides, *Chem. Geol*, 1997, vol. 135, pp. 307–324.

Distler, V.V., Mitrofanov, G.L., and Nemerov, V.K., Modes of occurrence of platinum group elements and their origin in the Sukhoi Log gold deposit, *Geol. Ore Deposits*, 1996, vol. 38, no. 6, pp. 413–428.

Goryachev, N.A., Budyak, A.E., Tarasova, Y.I., Ignat'ev, A.V., and Velivetskaya, T.A., A case history of applying in situ

analysis of the sulfur isotopic compositions of sulfides from ores of the largest deposits in the Bodaibo synclinorium (Eastern Siberia), *Dokl. Earth Sci*, 2019, vol. 484, no. 2, pp. 156–159.

Hall, A.J., Pyrite–pyrrhotine redox reactions in nature, *Mineral. Mag.*, 1986, vol. 50,pp. 223–229.

Hamor, T., The occurrence and morphology of sedimentary pyrite, *Geologica Hungarica*, 1994, vol. 37, nos. 1–2, pp. 153–181.

Ignatiev, A.V., Velivetskaya, T.A., Budnitskiy, S.Y., Yakovenko, V.V., Vysotskiy, S.V., and Levitskii, V.I., Precision analysis of multisulfur isotopes in sulfides by femtosecond laser ablation GC-IRMS at high spatial resolution, *Chem. Geol*, 2018, vol. 493, pp. 316–326.

Ivanov, A.I., *Zoloto Baikalo-Patoma (geologiya, orudenenie, perspektivy)* (Gold of Baikal–Patom (Geology, Mineralization, Prospects)), Moscow: TsNIGRI, 2014.

Ivanov, A.V., Vanin, V.A., Demonterova, E.I., Gladkochub, D.P., Donskaya, T.V., and Gorovoy, V.A., Application of the "no fool's clock" to dating the Mukodek gold field, Siberia, Russia, *Ore Geol. Rev.*, 2015, vol. 69, pp. 352–359.

Kretschmar, U. and Scott, S.D., Phase relations involving arsenopyrite in the system Fe-As-S and their application, *Can. Mineral.*, 1976, vol. 14, pp. 364–386.

Kryazhev, S.G., Ustinov, V.I., and Grinenko, V.A., Fluid regime at the Sukhoi Log gold deposit: isotopic evidence, *Geochem. Int.*, 2009, vol. 47, no. 10, pp. 1041–1049.

Kucherenko, I.V., Gavrilov, R.Yu., Martynenko, V.G., and Verkhozin, A.V., Petrological and geochemical features of rock wall metasomatism in the Verninsky gold ore deposit (Lensky district), *Bull. Tomsk Polytechnic Univ.*, 2012, vol. 321, no. 1, pp. 22–33.

Large, R.R., Maslennikov, V.V., Robert, F.L., Danyushevsky, V., and Chang, Z., Multistage sedimentary and metamorphic origin of pyrite and gold in the giant Sukhoi Log deposit, Lena Goldfield, Russia, *Econ. Geol.*, 2007, vol. 102, pp. 1233–1267.

Laverov, N.P., Chernyshev, I.V., Chugaev, A.V., Bairova, E.D., Goltsman, Y.V., Distler, V.V., and Yudovskaya, M.A., Formation stages of the large-scale noble metal mineralization in the Sukhoi Log deposit, East Siberia: results of isotope-geochronological study, *Dokl. Earth Sci*, 2007, vol. 415, no. 1, pp. 810–814.

Lee, J.-Y., Marti, K., Severinghaus, J.P., Kawamura, K., Yoo, H.-S., Lee, J.B., and Kim, J.S., A redetermination of the isotopic abundances of atmospheric Ar, *Geochim. Cosmochim. Acta*, 2006, vol. 70, pp. 4507–4512.

Meffre, S., Large, R.R., Scott, R., Scott, R., Woodhead, Z.C., Gilbert, S.E., Danyshevsky, L.D., Maslenikov, V.V., and Hergt, J.M., Age and pyrite Pb isotopic composition of the giant Sukhoi Log sediment hosted gold deposit, Russia," *Geochim. Cosmochim. Acta*, 2008, vol. 72, pp. 2377–2391.

Neimark, L.A., Rytsk, E.Yu., Rizvanova, N.G., and Gorokhovsky, B.M., On polychronous genesis of Angara–Vitim batolith according to U-Pb data on zircon and sphene, *Dokl. Earth Sci.*, 1993, vol. 333, pp. 634–638.

Nemerov, V.K., Razvozzhaeva, E.A., Budyak, A.E., Stanevich, A.M., and Kornilova, T.A., Biogenic sedimentation factors of mineralization in the Neoproterozoic strata of the Baikal-Patom region, *Russ. Geol. Geophys.*, 2010, vol. 51, no. 5, pp. 572–586.

Palenova, E.E., Belogub, E.V., Novoselov, K.A., Maslennikov, V.V., Kotlyarov, V.A., Blinov, I.A., Plotinskaya, O.Y., Griboedova, I.G., and Kuzmenko, A.A., Chemical evolution of pyrite at the Kopylovsky and Kavkaz black shale-hosted gold deposits, Bodaybo district, Russia: evidence from EPMA and LA-ISP-MS Data, *Geol. Ore Deposits*, 2015, vol. 57, no. 1, pp. 64–84.

Petrov, B.V. and Makrygina, V.A., *Geokhimiya regional'nogo metamorfizma I ul'trametamorfizma* (Geochemistry of Regional Metamorphism and Ultrametamorphism), Novosibirsk: Nauka, 1975.

Powerman, V., Shatsillo, A., Chumakov, N., Kapitonov, I., and Hourigan, J., Interaction between the Central Asian Orogenic Belt (CAOB) and the Siberian craton as recorded by detrital zircon suites from Transbaikalia, *Precambrian Res.*, 2015, vol. 267, no. 1, pp. 39–71.

Ramdohr, P., *The Ore Minerals and their Intergrowths*, Pergamon, 1969.

Rusinov, V.L., Borisovsky, S.E., Rusinova, O.V., Kryazhev, S.G., Shchegolkov, Yu.V., and Alysheva, E.I., Wall-rock metasomatism of carbonaceous terrigenous rocks in the Lena gold district, *Geol. Ore Deposits*, 2008, vol. 50, no. 1, pp. 1–40.

Stanevich, A.M., Mazukabzov, A.M., Gladkochub, D.P., Donskaya, T.V., Kornilova, T.A., Postnikov, A.A., Nemerov, V.K., and Pisarevsky, S.A., Northern segment of the Paleoasian ocean: Neoproterozoic deposition history and geodynamics, *Russ. Geol. Geophys.*, 2007, vol. 48, no. 1, pp. 46–60.

Tarasova, Yu.I., Budyak, A.E., Chugaev, A.V., Goryachev, N.A., Tauson, V.L., Skuzovatov, S.Yu., Reutsky, V.N., Abramova, V.D., Gareev, B.I., Bryukhanova, N.N., and Parshin, A.V., Mineralogical and isotope-geochemical ($\delta^{13}C$, $\delta^{34}S$, and Pb–Pb) characteristics of the Krasniy gold mine (Baikal–Patom Highlands): constraining ore-forming mechanisms and the model for Sukhoi Log-type deposits, *Ore Geol. Rev.*, 2020, no.2, pp. 128–146.

Tauson, V.L., Nemerov, V.K., Razvozzhaeva, E.A., Spiridonov, A.M., Lipko, S.V., and Budyak, A.E., Paragenetic relationships between pyrite, carbon, and gold at the Sukhoi Log deposit and typomorphism of the pyrite surface, *Dokl. Earth Sci.*, 2009, vol. 426, no. 1, pp. 690–694.

Tsygankov, A.A., *Magmaticheskaya evolyutsiya Baikalo-Muiskogo vulkanoplutonicheskogo poyasa v pozdnem dokembrii* (Magmatic Evolution of the Baikal-Muya Volcanoplutonic Belt in the Late Precambrian), Novosibirsk: GIN SB RAS, 2005.

Tsygankov, A.A., Litvinovsky, B.A., Jahn, B.M., Reichow, M.K., Liu, D.Y., Larionov, A.N., Presnyakov, S.L., Lepekhina, Y.N., and Sergeev, S.A., Sequence of magmatic events in the Late Paleozoic of Trans-Baikal region, Russia (U-Pb isotope dating). *Russ. Geol. Geophys.*, 2010, vol. 51, no. 9, pp. 972–994.

Vagina, E.A., Composition of fluid inclusions of the Chertovo Koryto gold deposit, In: *Materialy XV Vserossiskoi Konferentsii po termobarogeokhimii* (Proc. XV All-Russ.

Conf. on Thermobarogeochemistry), Moscow: IGEM RAS, 2012, pp. 23–24.

Velivetskaya, T.A., Ignatiev, A.V., Yakovenko, V.V., and Vysotskiy, S.V., An improved femtosecond laser-ablation fluorination method for measurements of sulfur isotopic anomalies $\delta^{33}S$ and $\delta^{36}S$) in sulfides with high precision, *Rapid Commun. Mass. Spectrom.*, vol. 33,no. 22, pp., 1722–1729.

Vermeesch, P., IsoplotR: A free and open toolbox for geochronology, *Geosci. Front.*, 2018, no. 9, pp. 1479–1493.

Xu, N., Wu, C., Li, S., Xue, B., He, X., Yu, Y., and Liu, J., LA-ICP-MS in situ analyses of the pyrites in Dongyang gold deposit, Southeast China: Implications to the gold mineralization, *China Geol.*, 2020, no. 1, pp. 1–17.

Yapaskurt, O.V., The aspects of the post-sedimental lithogenesis theory, *Litosfera*, 2005, no. 3, pp. 3–30.

Yudovskaya, M.A., Distler, V.V., Mokhov, A.V., Rodionov, N.V., Antonov, A.V., and Sergeev, S.A., Relationship between metamorphism and ore formation at the Sukhoi Log gold deposit hosted in black slates from the data of U-Th-Pb isotopic SHRIMP-dating of accessory minerals, *Geol. Ore Deposits*, 2011, vol. 53, no. 1, pp. 27–57.

Yudovskaya, M.A., Distler, V.V., Prokofiev, V.Yu., and Akinfiev, N.N., Gold mineralization and orogenic metamorphism in the Lena province of Siberia as assessed from Chertovo Koryto and Sukhoi Log deposits, *Geosci. Front.*, 2016, vol. 7, no. 3, pp. 453–481.

Zorin, Yu.A., Mazukabzov, A.M., and Gladkochub, D.P., The Silurian age of the major orogenic deformations of Riphean rocks in the Baikal–Patom zone, *Dokl. Earth Sci.*, 2008, vol. 463, no. 2, pp. 1235–1239.

Translated by I. Baksheev